

# Magnetic phase diagram of three-dimensional diluted Ising antiferromagnet

## $\text{Ni}_{0.8}\text{Mg}_{0.2}(\text{OH})_2$

Masatsugu Suzuki<sup>1\*</sup>, Itsuko S. Suzuki<sup>1†</sup>, Tedmann M. Onyango<sup>1</sup> and Toshiaki Enoki<sup>2</sup>

<sup>1</sup>*Department of Physics, State University of New York at Binghamton, Binghamton, New York 13902-6016, USA*

<sup>2</sup>*Department of Chemistry, Tokyo Institute of Technology, Meguro-ku, Tokyo 152-8551*

*H-T* diagram of 3D diluted Ising antiferromagnet  $\text{Ni}_c\text{Mg}_{1-c}(\text{OH})_2$  with  $c = 0.8$  has been determined from measurements of SQUID DC magnetization and AC magnetic susceptibility. At  $H = 0$ , this compound undergoes two magnetic phase transitions: an antiferromagnetic (AF) transition at the Néel temperature  $T_N$  ( $= 20.7$  K) and a reentrant spin glass (RSG) transition at  $T_{RSG}$  ( $\approx 6$  K). The *H-T* diagram consists of the RSG, spin glass (SG), and AF phases. These phases meet a multicritical point  $P_m$  ( $H_m = 42$  kOe,  $T_m = 5.6$  K). The irreversibility of susceptibility defined by  $\delta$  ( $= \chi_{FC} - \chi_{ZFC}$ ) shows a negative local minimum for  $10 \leq H \leq 35$  kOe, suggesting the existence of possible glassy phase in the AF phase. A broad peak in  $\delta$  and  $\chi''$  at  $H \geq 20$  kOe for  $T_N(c = 0.8, H) \leq T \leq T_N(c = 1, H = 0)$  ( $= 26.4$  K) suggests the existence of the Griffiths phase.

KEYWORDS: spin glass, Griffiths phase, random magnet

### 1. Introduction

The static and dynamics of Ising random spin systems present some of the most intriguing problems in magnetism.<sup>1)</sup> There are two types of spin ordering in Ising random spin systems that have attracted continuing interest for two decades: Ising spin glass (SG) and random-field Ising model (RFIM). The ordered phase of both cases is characterized by the irreversibility and the metastability due to multiple minima of the free-energy surface. The spin glass behavior is realized in random Ising spin systems with competing exchange interaction. The RFIM problems have been extensively discussed from a theoretical view point.<sup>1-3)</sup> Experimentally it is impossible to create random fields on a microscopic scale. However, the RFIM can be realized in a diluted Ising antiferromagnet in an uniform external magnetic field ( $H$ ).<sup>3)</sup> The random-field strength is predicted to be proportional to  $H$ .

In this paper we study the nature of glassy phases in a three-dimensional (3D) diluted Ising antiferromagnet  $\text{Ni}_c\text{Mg}_{1-c}(\text{OH})_2$  with  $c = 0.8$  in the presence of  $H$ . This compound shows two types of transition at  $H = 0$ : (i) the transition between the antiferromagnetic (AF) and paramagnetic (PM) phases at a Néel temperature  $T_N$  ( $= 20.7$  K) and (ii) the transition between the AF and reentrant spin glass (RSG) phases at a transition temperature  $T_{RSG}$  ( $\approx 6$  K).<sup>4)</sup> The present work has been motivated by the following three theoretical predictions on various types of glassy phases. The first is the prediction for the spin glass phase related to the AF system with RSG phase in an uniform  $H$ . The magnetic phase (*H-T*) diagram of an AF-based RSG (AF-RSG) system has been theoretically studied by Takayama<sup>5)</sup> and Fyodorov et al.<sup>6)</sup> based on a molecular field theory (see §2). These theories predict that the *H-T* diagram consists of four phases, an AF phase, a RSG phase, a pure

SG phase, and a PM phase. These four phases meet at a new multicritical point. An AF-RSG transition temperature  $T_{RSG}(H)$  tends to increase with increasing  $H$ . The extrapolation of the phase boundary between the AF phase and PM phase to the low- $T$  side separates the RSG phase and SG phase, where the SG phase is in the higher- $H$  side. The second is the prediction for the glassy phase in a 3D diluted Ising antiferromagnet under an uniform  $H$  as a realization of the RFIM. It has been theoretically predicted that a glassy phase exists between the PM phase and AF phase in the *H-T* phase diagram of the 3D diluted Ising antiferromagnet in an uniform field  $H$ .<sup>7-11)</sup> There are two-types of states at the same  $H$  and  $T$ : zero-field (ZFC) and field-cooled (FC) states. The FC state is obtained upon cooling of the system at constant  $H$  and the ZFC state is obtained by first cooling at  $H = 0$  and then applying  $H$  and reheating. The ZFC state (which has long range order) has a lower free energy in the AF phase, while the FC state (the multi-domain state) has a lower free energy in the glassy phase.<sup>12)</sup> However, it is not clear whether the glassy phase is regarded as a truly separate phase or simply as having long relaxation times due to domain-wall pinning. Experimentally it is expected that the ZFC magnetization  $M_{ZFC}$  is larger than the FC magnetization  $M_{FC}$  in the glass phase ( $H > H_{crit}$ ) and that the opposite inequality holds for  $H < H_{crit}$ ,<sup>8)</sup> where the crossover line between the glassy phase and the AF phase is denoted by  $H = H_{crit}(T)$ . This may be an useful experimental signature of the onset of the glassy phase. The third is a so-called Griffiths phase conjecture<sup>13)</sup> which is based on the idea of local phase transitions in a diluted system due to the finite probability of arbitrarily large pure and differently diluted clusters. The Griffiths phase is the phase of the slowly fluctuating spins that exists in the paramagnetic region  $T_N(c, H) \leq T \leq T_N(c = 1, H)$ , where  $T_N(c, H)$  is the Néel temperature of the system with the concentration  $c$ .

\*E-mail address: suzuki@binghamton.edu

†E-mail address: itsuko@binghamton.edu

As far as we know, there has been at least one report in a 3D diluted Ising antiferromagnet ( $\text{Fe}_{0.552}\text{Mg}_{0.448}\text{Cl}_2$ ),<sup>14)</sup> which supports the first prediction. At  $H = 0$  this compound undergoes a PM-AF transition at  $T_N (= 7.5 \text{ K})$  and AF-RSG transition at  $T_{RSG} (\approx 3.0 \text{ K})$ . The RSG phase is a mixed phase where SG behavior and AF long range-order coexist.<sup>15)</sup> An uniform magnetic field  $H$  along the  $c$  axis enlarges the domain of existence of the RSG phase in the  $(T, H)$  plane for  $H < 5 \text{ kOe}$ :  $T_{RSG}(H)$  increases with increasing  $H$  and meets with  $T_N(H)$  at a multicritical point. Such an increase of  $T_{RSG}$  may give an experimental evidence for the random field (RF) effect.<sup>14)</sup> The existence of the Griffiths phase has been reported in pure  $\text{FeCl}_2$ <sup>16)</sup> and  $\text{Fe}_{0.47}\text{Zn}_{0.53}\text{F}_2$ .<sup>17)</sup> Binek et al.<sup>16,17)</sup> have shown that there exist domain-like antiferromagnetic correlations in the temperature range  $T_N(c, H) \leq T \leq T_N(c = 1, H = 0)$ , when  $H$  is applied along the  $c$  axis. As far as we know, there has been no report on the Griffiths phase in  $\text{Fe}_c\text{Mg}_{1-c}\text{Cl}_2$  with  $0.5 \leq c \leq 0.61$ . We note that the existence of the cluster-ordered Griffiths phase in  $\text{Ni}_c\text{Mg}_{1-c}(\text{OH})_2$  has been claimed by Deguchi et al.<sup>18)</sup> from their SQUID DC magnetization measurement and by Zenmyo et al.<sup>19)</sup> from proton nuclear magnetic resonance.

In this paper we have determined the  $H$ - $T$  phase diagram of  $\text{Ni}_c\text{Mg}_{1-c}(\text{OH})_2$  with  $c = 0.8$  from the measurements of DC magnetic susceptibility and AC magnetic susceptibility ( $1.9 \leq T \leq 30 \text{ K}$ ,  $0 \leq H \leq 48 \text{ kOe}$ ,  $0.05 \leq f \leq 1000 \text{ Hz}$ ). We show that for low  $H$  ( $0 \leq H \leq 3 \text{ kOe}$ ) the difference  $\delta (= \chi_{FC} - \chi_{ZFC})$  is positive for any  $T$  and exhibits two step-like increases at different temperatures with decreasing  $T$ : a weak irreversibility at  $T$  just below  $T_N(H)$  due to a possible RF effect and a strong irreversibility at  $T_{RSG}(H)$  due to the RSG phase. In contrast,  $\delta$  for  $10 \leq H \leq 48 \text{ kOe}$  is negative below  $T_N(H = 0)$ , suggesting the possible glassy phase between the PM and AF phases as a result of RFIM. We find the strong  $H$  dependence of the absorption  $\chi''$  at low  $T$ , showing a peak at  $H \approx 42 \text{ kOe}$ , suggesting the separation between the RSG and SG phase at low  $T$ . We also find the Griffiths phase in  $\text{Ni}_{0.8}\text{Mg}_{0.2}(\text{OH})_2$ . The absorption  $\chi''$  shows a very broad peak at  $T$  between  $T_N(c = 0.8, H)$  and  $T_N(c = 1, H = 0) (= 26.4 \text{ K})$ . The frequency dependence of  $\chi''$  vs  $T$  is also examined at  $H = 30$  and  $40 \text{ kOe}$  to determine the average relaxation time  $\tau_G$ .

## 2. Background: $H$ - $T$ phase diagram for the AF based RSG systems

Here we present a simple review on the theory of the  $H$ - $T$  diagram for an AF based reentrant spin glass (AFRSG). According to Takayama,<sup>5)</sup> the system consists of two Ising spin glass sublattices  $\{S_{1i}\}$  and  $\{S_{12}\}$ , which are coupled by the intra-sublattice exchange interaction  $I_{ij}$  and are coupled antiferromagnetically on average through the inter-sublattice exchange interactions  $J_{ij}$ . These interactions are assumed to be independent Gaussian random variables with the distribution of the mean value  $I_0/N$  and  $-J_0/N$  and variances  $I^2/N$  and  $J^2/N$ , where  $I_0 > 0$  and  $J_0 > 0$ ,  $I_0 = r_F J_0$ ,  $I = rJ$ , and  $N$  is the number of spins in each sublattice. Figures 1(a) and (b) show the  $H$ - $T$  diagram of the AFRSG system

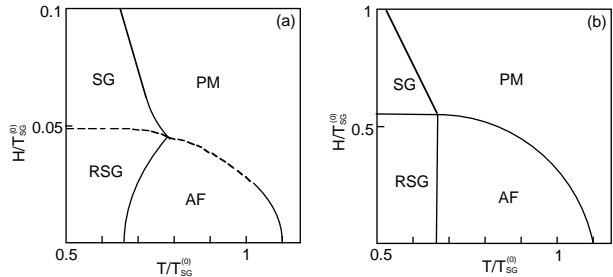


Fig. 1. The  $H$ - $T$  diagram predicted from the mean-field theory<sup>5)</sup> for (a) an enhanced AF-RSG system with  $r = r_F = 5$  and  $r_N = 1.1$ , and (b) a simple AF-RSG system with  $r = r_F = 0$  and  $r_N = 1.1$ . The dashed line in (a) is of the first order. The definition of  $r$ ,  $r_F$ ,  $r_N$ , and  $T_{SG}^{(0)}$  is given in the text.

with (a)  $r = r_F = 5$  and  $r_N = 1.1$  and (b)  $r = r_F = 0$  and  $r_N = 1.1$ , respectively, where  $T_N^{(0)} = (1 + r_F)J_0$  and  $T_{SG}^{(0)} = (1 + r^2)^{1/2}J$ , and  $r_N = T_N^{(0)}/T_{SG}^{(0)}$ . There are four phases: PM, AF, RSG, and pure SG phases. In the case of (a), there is a crossover from the second order transition to the first order transition on the boundary between the PM and AF phases. The boundary between the SG and RSG phases is also of the first order. The AF-RSG transition temperature  $T_{RSG}$  increases with increasing  $H$ . The case (b) ( $r = r_F = 0$ ) corresponds to the model discussed by Fyodorov et al.<sup>6)</sup>

## 3. Experimental procedure

Powdered sample of  $\text{Ni}_{0.8}\text{Mg}_{0.2}(\text{OH})_2$  used in the present work was the same as those used in the previous work.<sup>4)</sup> The detail of sample preparation was reported before.<sup>20)</sup> The DC magnetization and AC magnetic susceptibility were measured using a SQUID (superconducting quantum interference device) magnetometer (Quantum Design, MPMS XL-5).

(i) *SQUID DC magnetization*. Before setting up a sample at 298 K, a remanent magnetic field in a superconducting magnet was reduced to one less than 3 mOe using an ultra low field capability option of the SQUID magnetometer. For convenience, hereafter this remanent field is denoted as the state of  $H = 0$ . The sample was cooled from 298 to 1.9 K at  $H = 0$ . Then an external magnetic field  $H$  ( $1 \text{ Oe} \leq H \leq 48 \text{ kOe}$ ) was applied at 1.9 K. A zero-field cooled magnetization ( $M_{ZFC}$ ) was measured with increasing  $T$  from 1.9 to 30 K. After the ZFC measurement, the sample was heated and kept at 100 K for 20 minutes. It was again cooled to 30 K in the presence of the same  $H$ . A field-cooled magnetization ( $M_{FC}$ ) was measured with decreasing  $T$  from 30 to 1.9 K.

(ii) *SQUID AC magnetic susceptibility*. The frequency ( $f$ ) dependence of  $\chi'$  and  $\chi''$  was measured at various  $T$ . The sample was cooled from 298 to 1.9 K at  $H = 0$ . An external magnetic field ( $H = 30$  and  $40 \text{ kOe}$ ) was applied at 1.9 K. Then both  $\chi'$  and  $\chi''$  were simultaneously measured as a function of frequency ( $0.1 \text{ Hz} \leq f \leq 100 \text{ Hz}$ ) at fixed  $T$ .  $T$  is increased by  $\Delta T = 0.5 \text{ K}$  after each frequency scan. The amplitude of AC magnetic field  $h$  was 3 Oe. The  $T$  dependence of  $\chi'$  and  $\chi''$  was also measured in the presence of various  $H$ , where  $f = 1 \text{ Hz}$  and  $h =$

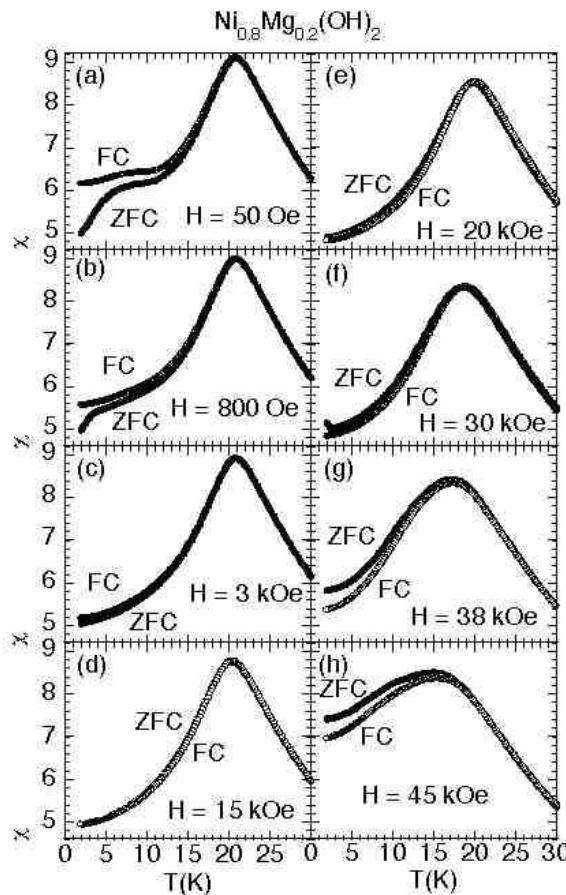


Fig. 2. (a) - (h)  $T$  dependence of  $\chi_{ZFC}$  ( $= M_{ZFC}/H$ ) ( $\bullet$ ) and  $\chi_{FC}$  ( $= M_{FC}/H$ ) ( $\circ$ ) for  $\text{Ni}_{0.8}\text{Mg}_{0.2}(\text{OH})_2$  at various  $H$  ( $50 \text{ Oe} \leq H \leq 45 \text{ kOe}$ ).

3 Oe. The sample was cooled from 298 to 1.9 K in  $H = 0$ . Then  $\chi'$  and  $\chi''$  were simultaneously measured with increasing  $T$  from 1.9 to 30 K in the presence of fixed  $H$ . After each  $T$  scan,  $H$  was changed at 30 K and  $T$  was decreased from 30 to 1.9 K. Then the measurement was repeated at the same  $H$ .

#### 4. Result

##### 4.1 $\chi_{ZFC}$ and $\chi_{FC}$

Figure 2 shows the  $T$  dependence of  $\chi_{ZFC}$  ( $= M_{ZFC}/H$ ) and  $\chi_{FC}$  ( $= M_{FC}/H$ ) for  $\text{Ni}_{0.8}\text{Mg}_{0.2}(\text{OH})_2$  at various  $H$  ( $50 \text{ Oe} \leq H \leq 45 \text{ kOe}$ ). Figure 3 shows the  $T$  dependence of the difference  $\delta$  ( $= \chi_{FC} - \chi_{ZFC}$ ) at various  $H$ . At  $H = 50$  Oe both  $\chi_{ZFC}$  and  $\chi_{FC}$  exhibit a peak at 20.8 K. The deviation of  $\chi_{ZFC}$  from  $\chi_{FC}$  starts to occur below 22 K, indicating the positive sign of  $\delta$ . Note that  $\delta$  increases in two steps with decreasing  $T$ : a weak change near 22 K and a strong change below 5.8 K. As will be discussed in §5.4, the strong irreversibility is related to the RSG ordering,<sup>4)</sup> while the weak irreversibility is due to the RF effect. For simplicity  $T_{RSG}$  and  $T_{RF}$  are defined as temperatures at which  $\delta$  starts to show strong and weak irreversibility, respectively. For  $100 \text{ Oe} \leq H < 3 \text{ kOe}$ , similar step-like changes in  $\delta$  are also observed at  $T_{RSG}$  and  $T_{RF}$ . Here  $T_{RSG}$  decreases with increasing  $H$  ( $T_{RSG} = 5.8 \text{ K}$  at 50 Oe and  $3.0 \text{ K}$  at 3 kOe), while  $T_{RF}$  seems to be independent of  $H$  ( $T_{RF}$

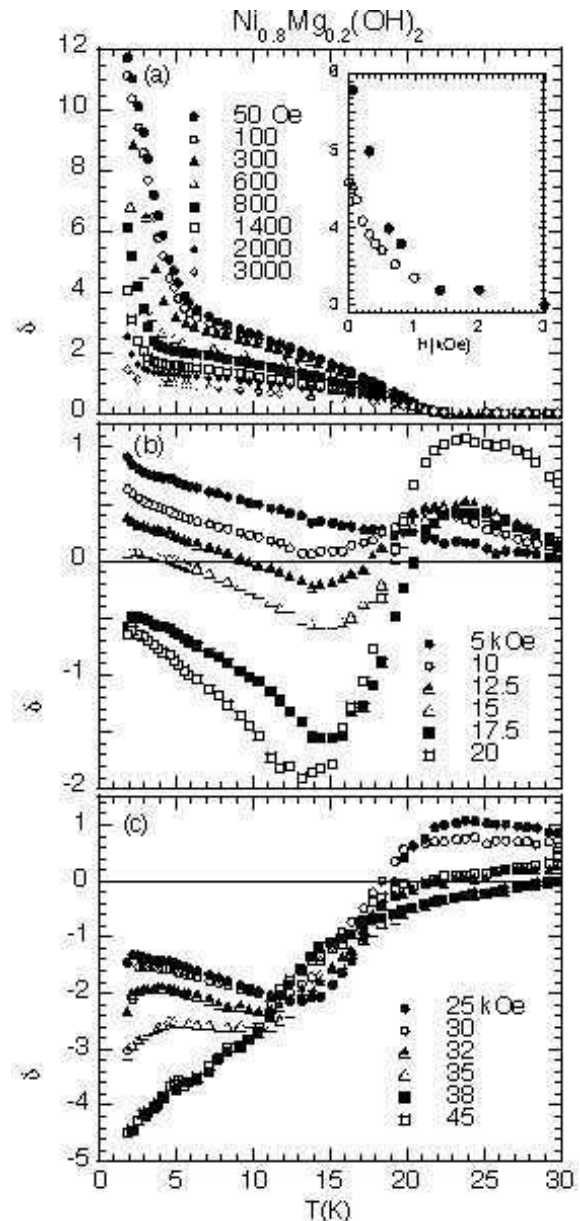


Fig. 3. (a)-(c)  $T$  dependence of  $\delta$  ( $= \chi_{FC} - \chi_{ZFC}$ ) at various  $H$  ( $50 \text{ Oe} \leq H \leq 45 \text{ kOe}$ ). The inset of (a) shows the  $H$  dependence of  $T_{RSG}$ .  $T_{RSG}$  is defined as a temperature at which  $\delta$  shows a strong irreversibility ( $\bullet$ ) or  $\chi''$  has a peak ( $\circ$ ).

$= 22.0 - 22.4 \text{ K}$ ) and is a little higher than the Néel temperature  $T_N$  ( $c = 0.8, H = 0$ ) ( $= 20.7 \text{ K}$ ). The  $H$  dependence of  $T_{RSG}$  thus obtained is plotted in the inset of Fig. 3(a).

The magnetic behavior for  $H \geq 10 \text{ kOe}$  is rather different from that for  $H \leq 3 \text{ kOe}$ . At  $H = 20 \text{ kOe}$ ,  $\chi_{ZFC}$  and  $\chi_{FC}$  exhibit a peak at 19.8 and 20.0 K, respectively. The sign of  $\delta$  changes from positive to negative around 18.9 K as  $T$  decreases, implying that the value of  $\chi_{ZFC}$  is larger than that of  $\chi_{FC}$ . The difference  $\delta$  shows a negative local minimum at a characteristic temperature  $T_{min}$  ( $= 13.1 \text{ K}$ ). At  $H = 30 \text{ kOe}$ ,  $\chi_{ZFC}$  and  $\chi_{FC}$  exhibit a peak at 18.5 and 18.8 K, respectively. The sign of  $\delta$  changes from positive to negative at 18.3 K as  $T$  decreases. The difference  $\delta$  shows a negative local minimum at 11.7 K. A drastic decrease in  $\delta$  with decreasing  $T$  is seen below

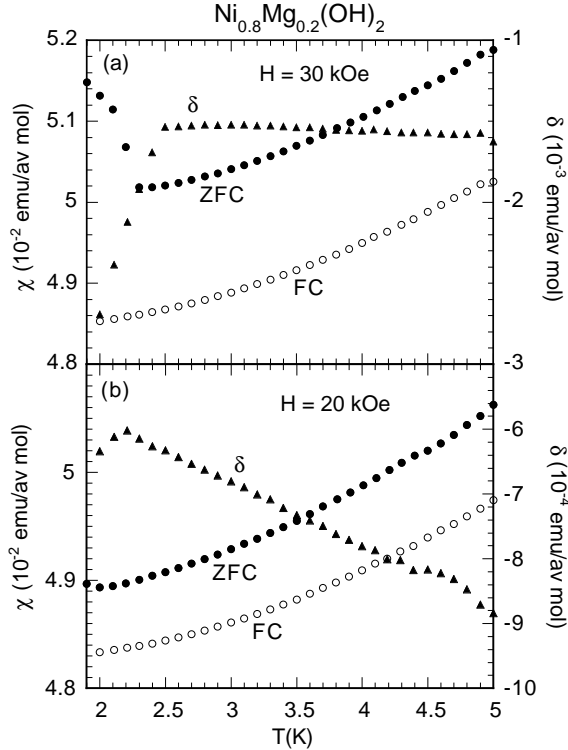


Fig. 4. (a) and (b)  $T$  dependence of  $\chi_{ZFC}$ ,  $\chi_{FC}$ , and  $\delta$  at  $H = 30$  and 20 kOe around  $T_\delta$ .

a characteristic temperature  $T_\delta$  ( $= 2.5$  K). As shown in Figs. 3(b) and (c), the local minimum in  $\delta$  at  $T_{min}$  is observed for  $10 \leq H \leq 35$  kOe, and the drastic decrease in  $\delta$  below  $T_\delta$  is seen for  $15 \leq H \leq 35$  kOe. The value of  $T_{min}$  decreases with increasing  $H$ , while the value of  $T_\delta$  increases with increasing  $H$ :  $T_{min} = 15$  K at  $H = 10$  kOe, 10.2 K at  $H = 35$  kOe, and  $T_\delta = 2.2$  K at  $H = 15$  kOe, 4.2 K at  $H = 35$  kOe. The  $H$  dependence of  $T_{min}$  and  $T_\delta$  will be discussed in §5.4. For  $H \geq 38$  kOe,  $\delta$  becomes negative below 30 K and decreases with decreasing  $T$ . No anomaly in  $\delta$  is observed. We note that the positive local maximum of  $\delta$  around 23.7 K observed for  $12.5 \leq H \leq 25$  kOe is related to the occurrence of the Griffiths phase (see §5.5). Figures 4 (a) and (b) show the  $T$  dependence of  $\chi_{ZFC}$ ,  $\chi_{FC}$ , and  $\delta$  at  $H = 20$  and 30 kOe around  $T_\delta$ . The susceptibility  $\chi_{ZFC}$  at  $H = 30$  kOe drastically increases with decreasing  $T$  below  $T_\delta$ , leading to the decrease of  $\delta$ .

Figures 5(a) and (b) show the  $T$  dependence of  $d\chi_{FC}/dT$  for each  $H$ , which is calculated based on the data of  $\chi_{FC}$  vs  $T$ . For  $H = 50$  Oe,  $d\chi_{FC}/dT$  shows two peaks at 5.2 and 17.9 K. The peak at low  $T$  disappears above 800 Oe. The peak at high  $T$  is well defined for  $H \leq 30$  kOe and is increasingly rounded, partly because of an increasing temperature interval where the critical slowing-down effect predominates. Note that the temperature at which  $d\chi_{FC}/dT$  is equal to zero coincides with the peak temperature of  $\chi_{FC}$ . Figures 5(c) and (d) show the  $T$  dependence of  $d\chi_{ZFC}/dT$  for each  $H$ , which is calculated based on the data of  $\chi_{ZFC}$  vs  $T$ . For  $H = 50$  Oe,  $d\chi_{ZFC}/dT$  shows two peaks at 3.4 and 17.80 K. The peak at low  $T$  shifts to the low- $T$  side with increasing

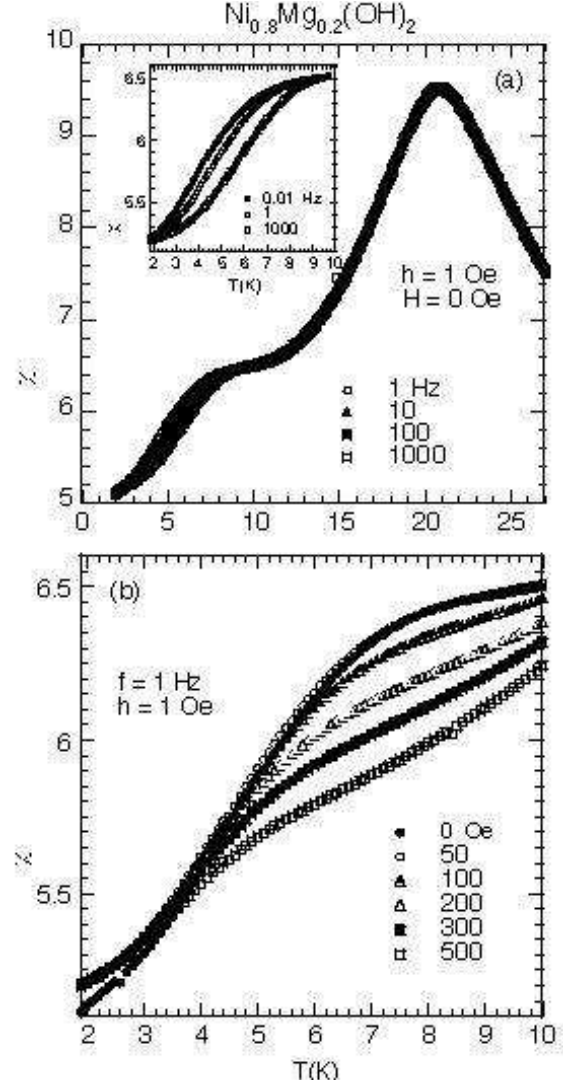


Fig. 6. (a)  $T$  dependence of  $\chi'$  at various  $f$ .  $h = 1$  Oe.  $H = 0$ .  
(b)  $T$  dependence of  $\chi'$  at various  $H$ .  $f = 1$  Hz.  $h = 1$  Oe.

$H$ . The peak at high  $T$  is increasingly rounded above 35 kOe. Similar behavior is observed in  $\text{Fe}_{0.46}\text{Zn}_{0.54}\text{F}_2$ ,<sup>21)</sup> where  $d\chi_{ZFC}/dT$  has a sharp peak at  $T_N(H)$  for  $H \leq 23$  kOe and a rounded peak for  $H \geq 40$  kOe. The  $H$  dependence of the peak temperature for  $\text{Ni}_{0.8}\text{Mg}_{0.2}(\text{OH})_2$  is well described by  $T_p(H) = T_p(H = 0) - AH^y$ , with  $T_p(H = 0) = 17.74 \pm 0.02$  K,  $A = (1.92 \pm 0.87) \times 10^{-8}$ , and  $y = 1.83 \pm 0.09$ .

#### 4.2 $\chi'(T, H)$

Figure 6(a) shows the  $T$  dependence of the dispersion  $\chi'$  at various  $f$ , where  $H = 0$  and  $h = 1$  Oe. The dispersion  $\chi'$  has a broad shoulder around 5-7 K and a sharp peak at 20.7 K. The shape of the shoulder is strongly dependent on  $f$ , while the shape of the peak is independent of  $f$ . Figure 6(b) shows the  $T$  dependence of  $\chi'$  at  $H = 0$  and at  $H$  (50-500 Oe), where  $f = 1$  Hz and  $h = 1$  Oe. The shoulder tends to disappear above 500 Oe. Figures 7(a) and (b) show the  $T$  dependence of  $\chi'$  at higher  $H$ , where  $h = 3$  Oe and  $f = 1$  Hz. The shoulder completely disappears at  $H = 2$  kOe. For  $H \leq 14$  kOe the peak slightly shifts to the low- $T$  side with increasing  $H$ . For

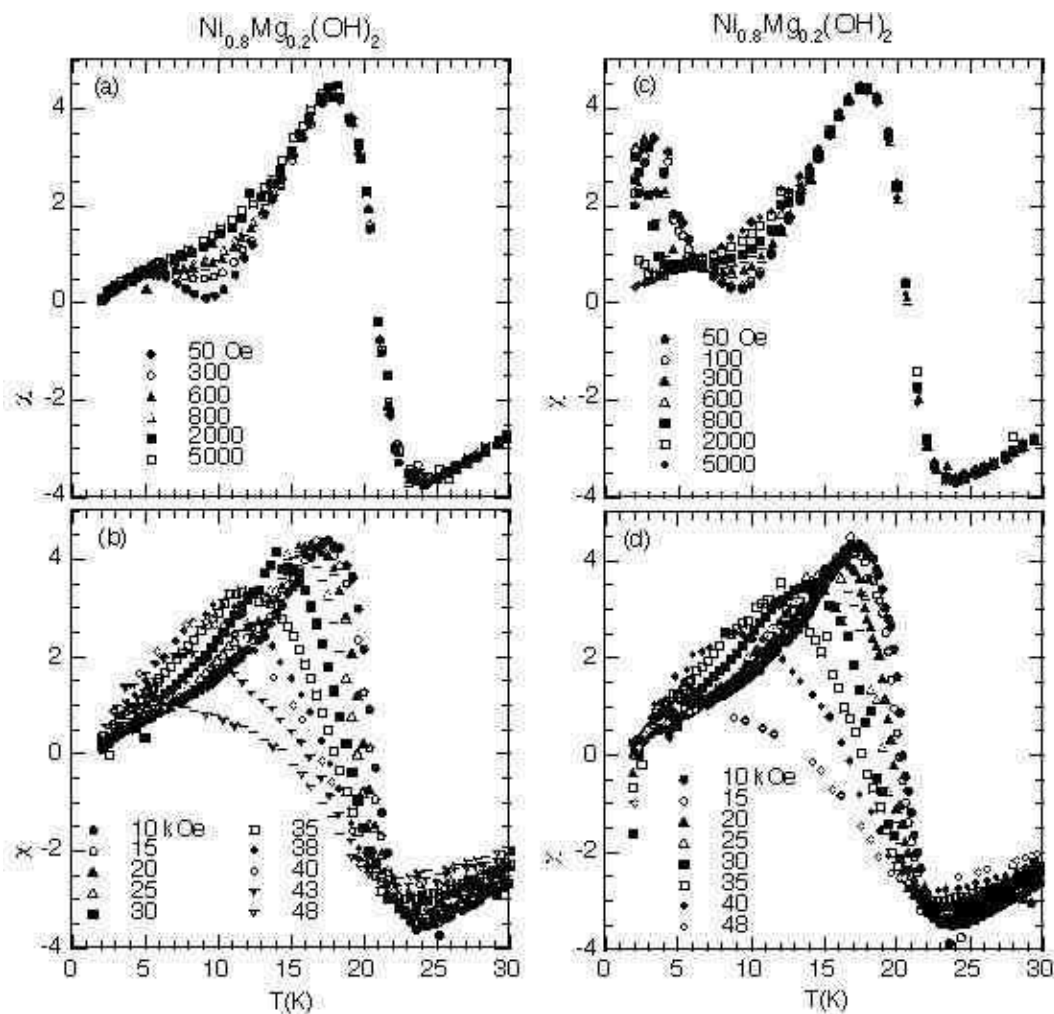


Fig. 5. (a) and (b)  $T$  dependence of  $d\chi_{FC}/dT$  for at various  $H$ . (c) and (d)  $T$  dependence of  $d\chi_{ZFC}/dT$  for at various  $H$ .

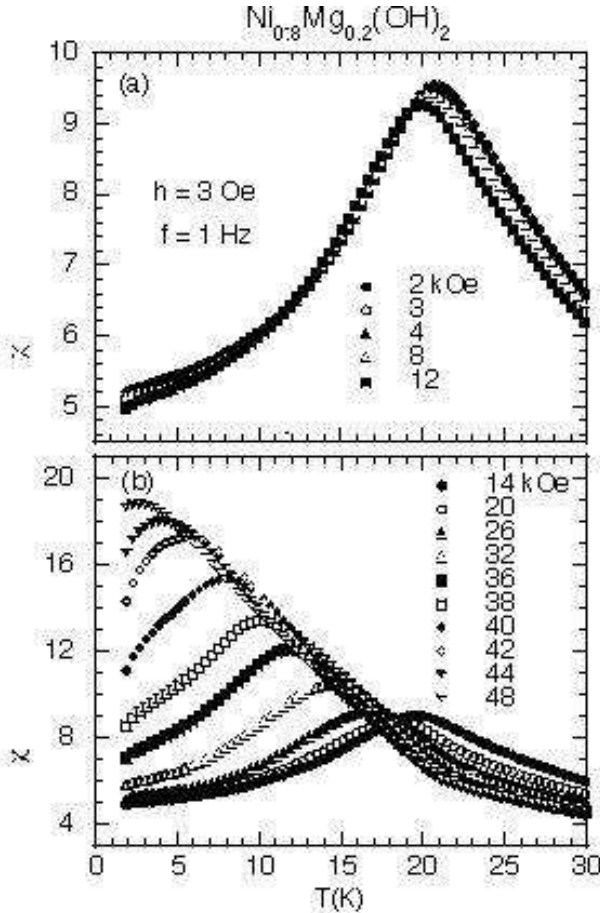


Fig. 7. (a) and (b)  $T$  dependence of  $\chi'$  at various  $H$ .  $f = 1$  Hz,  $h = 3$  Oe.

$H \geq 20$  kOe the peak drastically shifts to the low- $T$  side. As will be discussed in §5.1, it is reasonable to define the peak temperature of  $\chi'$  vs  $T$  as  $T_N(H)$ . The relation between  $T_N(H)$  and  $H$  leads to the  $H$ - $T$  phase diagram. We find that the curvature of  $H$  vs  $T$  changes from concave for  $H > 38$  kOe to convex for  $H < 38$  kOe. Note that there are two kinds of field-induced transitions for AF systems: the spin-flop transition for  $H'_E > H_A$  and the metamagnetic transition for  $H'_E < H_A$ . Here  $H'_E$  is the interplanar exchange field and  $H_A$  is the anisotropy field. The spin-flop transition occurs between the AF and spin-flop (SF) phases at  $H_{SF} = [H_A(2H'_E - H_A)]^{1/2}$ .<sup>22)</sup> The magnetization saturates at  $H_s = 2H'_E - H_A \approx 2H'_E$ . In contrast, the metamagnetic transition occurs between the AF and ferromagnetic (FM) phases at  $H = H'_E$ . It is considered that our system with  $c = 0.8$  undergoes the spin-flop transition rather than the metamagnetic transition. When  $H_s \approx 55$  kOe for  $c = 1$ <sup>23)</sup> and  $H_{SF}$  is assumed to be 38 kOe, we can estimate  $H'_E = 40.6$  kOe and  $H_A = 26.3$  kOe, satisfying the condition for the spin-flop transition. The value of  $H'_E$  thus obtained is larger than that ( $H'_E \approx 22.3$  kOe) reported by Enoki et al. for  $c = 1$ .<sup>20,23)</sup> The AF, the paramagnetic (PM) phase, and a possible SF phase merge at a critical point  $P_0$  ( $H_0 = 38$  kOe,  $T_0 = 10$  K). A line connecting between the critical point  $P_0$  and  $T = 20.8$  K at  $H = 0$  is a critical line  $H_c$  of the second order (see the definition of  $H_c$  and  $P_0$  in §5.2).

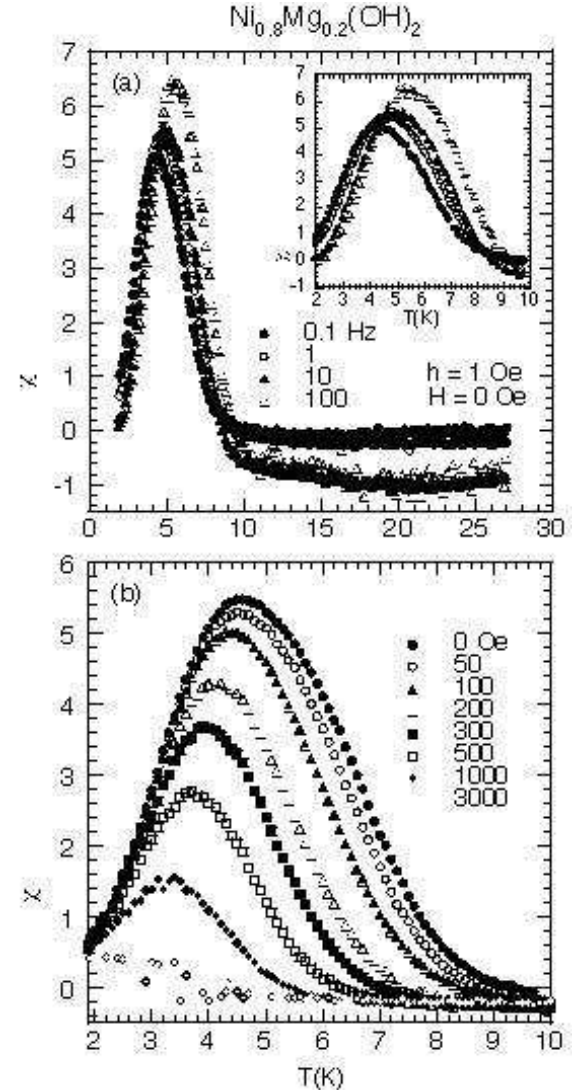


Fig. 8. (a)  $T$  dependence of  $\chi''$  at various  $f$ .  $h = 1$  Oe.  $H = 0$ .  
(b)  $T$  dependence of  $\chi''$  at various  $H$ .  $f = 1$  Hz.  $h = 1$  Oe.<sup>4)</sup>

This critical line is well described by

$$T_N(H) = T_N(H = 0) - AH^y, \quad (1)$$

with  $T_N(c = 0.8, H = 0) = 20.76 \pm 0.10$  K,  $A = (5.83 \pm 1.97) \times 10^{-9}$ , and  $y = 2.00 \pm 0.03$ . The index  $y$  is very close to the prediction from the molecular field theory.

#### 4.3 $\chi''(T, H)$

Figure 8(a) shows the  $T$  dependence of the absorption  $\chi''$  at various  $f$ , where  $H = 0$  and  $h = 1$  Oe. No anomaly is observed around  $T_N$ .<sup>4)</sup> A peak observed around 4.55 K is strongly dependent on  $f$ . This peak shifts to the high- $T$  side with increasing  $f$ . This peak is related to the RSG ordering. Figure 8(b) shows the  $T$  dependence of  $\chi''$  for at  $H = 0$  and at  $H$  ( $H = 50$  Oe - 3 kOe), where  $f = 1$  Hz and  $h = 1$  Oe. The peak shifts to the low- $T$  side with increasing  $H$ : 2.68 K at  $H = 2$  kOe and 2.3 K at  $H = 3$  kOe. It tends to disappear at  $H = 3$  kOe. In the inset of Fig. 3(a), for comparison, we show the  $H$  dependence of  $T_{RSG}$ , which is defined as the peak temperature for the data of  $\chi''$  vs  $T$ . Note that  $T_{RSG}$  from  $\delta$  is a little higher

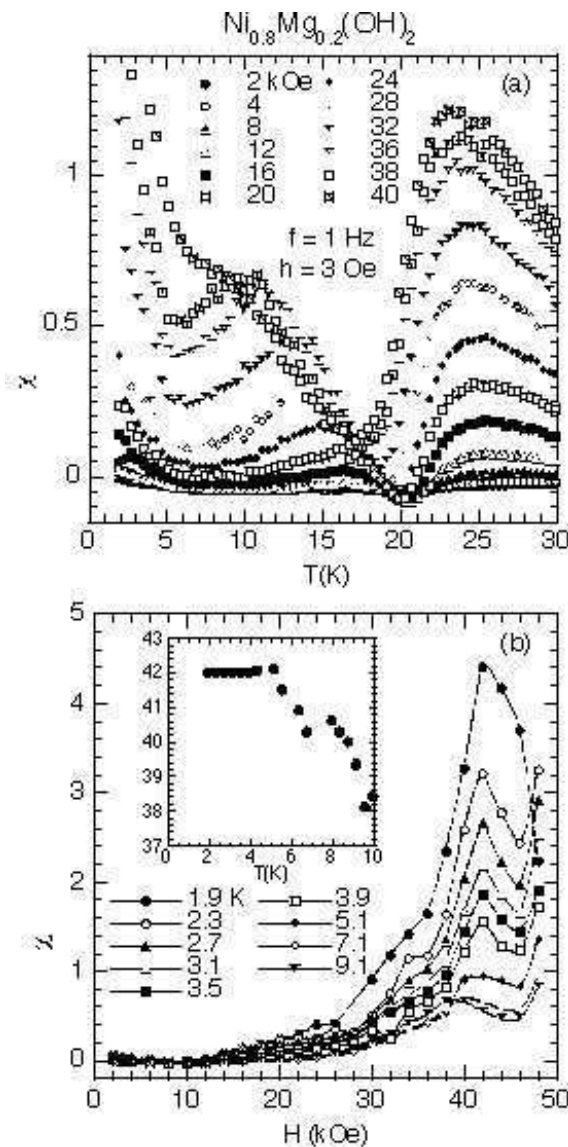


Fig. 9. (a)  $T$  dependence of  $\chi''$  at various  $H$ , (b)  $H$  dependence of  $\chi''$  at various  $T$ .  $f = 1$  Hz.  $h = 3$  Oe. The inset shows the plot of the peak field vs  $T$ .

than that from  $\chi''$  at the same  $H$ .

Figure 9(a) shows the  $T$  dependence of the absorption  $\chi''$  at higher  $H$ , where  $h = 3$  Oe and  $f = 1$  Hz. A strong divergence of  $\chi''$  for  $H \geq 40$  kOe is observed as  $T$  approaches zero. This is in contrast to a weak increase of  $\chi''$  for  $H \leq 30$  kOe with decreasing  $T$ . Figure 9(b) shows the  $H$  dependence of  $\chi''$  at various low  $T$ . The absorption  $\chi''$  drastically increases with increasing  $H$ , showing a sharp peak around 42 kOe. This result strongly suggests the transition between the RSG and a SG phases, as is predicted by Takayama<sup>5)</sup> for the AF-RSG systems (see Fig. 1).

As shown in Fig. 9(a)  $\chi''$  for  $12 \leq H \leq 40$  kOe exhibits a rather broad peak around 8.2 - 16.5 K, which is due to the PM-AF transition. The peak shifts to the low- $T$  side with increasing  $H$ : 16.5 K at  $H = 12$  kOe and 8.2 K at 40 kOe. This peak temperature is a little lower than the peak temperature of  $\chi'$  or  $T_N(H)$  at the same  $H$ . We also note another broad peak in  $\chi''$  at  $T$  above

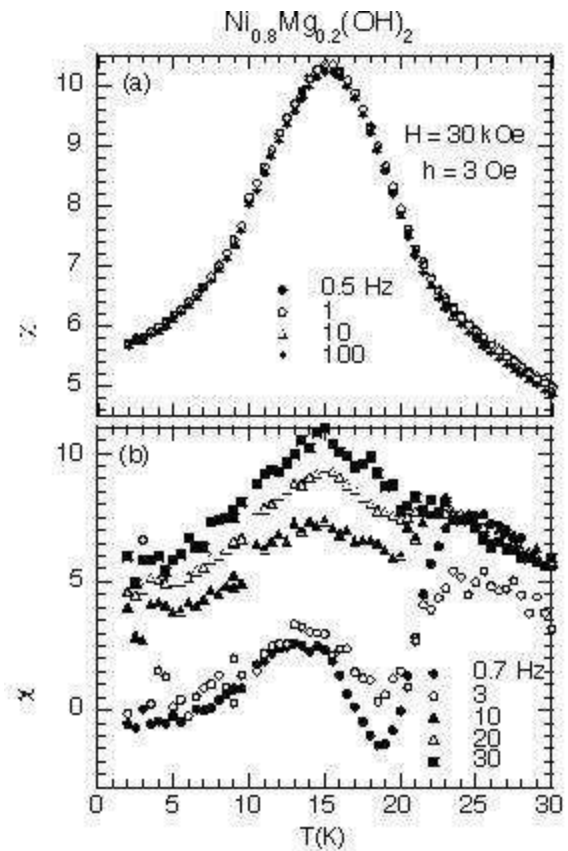


Fig. 10.  $T$  dependence of (a)  $\chi'$  and (b)  $\chi''$  at various  $f$  ( $0.5 \leq f \leq 100$  Hz).  $H = 30$  kOe.  $h = 3$  Oe.

$T_N(H)$  for  $H \geq 10$  kOe. The dispersion  $\chi'$  does not show any anomaly in the same region of the  $H$ - $T$  plane. The broad peak in  $\chi''$  shifts to the low- $T$  side with increasing  $H$ : 26.0 K at  $H = 10$  kOe and 22.3 K at  $H = 48$  kOe. This peak is not due to the ferromagnetic short-range fluctuations occurring in the same layer, since the peak temperature decreases with increasing  $H$ . This peak is related to the Griffiths phase. The absorption  $\chi''$  at  $H = 2$  kOe shows a local minimum at 21.1 K. This minimum survives up to 48 kOe: it shifts to the low- $T$  side with increasing  $H$ . The  $H$  dependence of local-minimum temperature is almost the same as that of the peak temperatures of  $\chi_{ZFC}$  and  $\chi_{FC}$ .

In order to investigate the nature of the Griffiths phase we have measured the  $f$  and  $T$  dependence of  $\chi'$  and  $\chi''$  at  $H = 30$  and 40 kOe. Figures 10(a) and (b) show the  $T$  dependence of  $\chi'$  and  $\chi''$  at  $H = 30$  kOe, respectively, where  $h = 3$  Oe and  $f$  is varied between 0.5 and 100 Hz. The dispersion  $\chi'$  has a single peak at 15.2 K, which is independent of  $f$ . In contrast,  $\chi''$  shows two peaks at 12.95 K and  $T_G \approx 25.1$  K at  $f = 0.5$  Hz. The peak at 25.1 K slightly shifts to the low- $T$  side with increasing  $f$  ( $T_G = 22.1$  K for  $f = 20$  Hz) and disappears for  $f \geq 30$  Hz. Figures 11(a) and (b) show the  $T$  dependence of  $\chi''$  at  $H = 40$  kOe, where  $h = 3$  Oe and  $f$  is varied between 0.5 and 100 Hz. The absorption  $\chi''$  at  $f = 0.5$  Hz shows a peak around 23.5 K. This peak shifts to the low- $T$  side with increasing  $f$  for  $0.5 \leq f \leq 3$  Hz and disappears above 20 Hz. It is predicted that the clusters

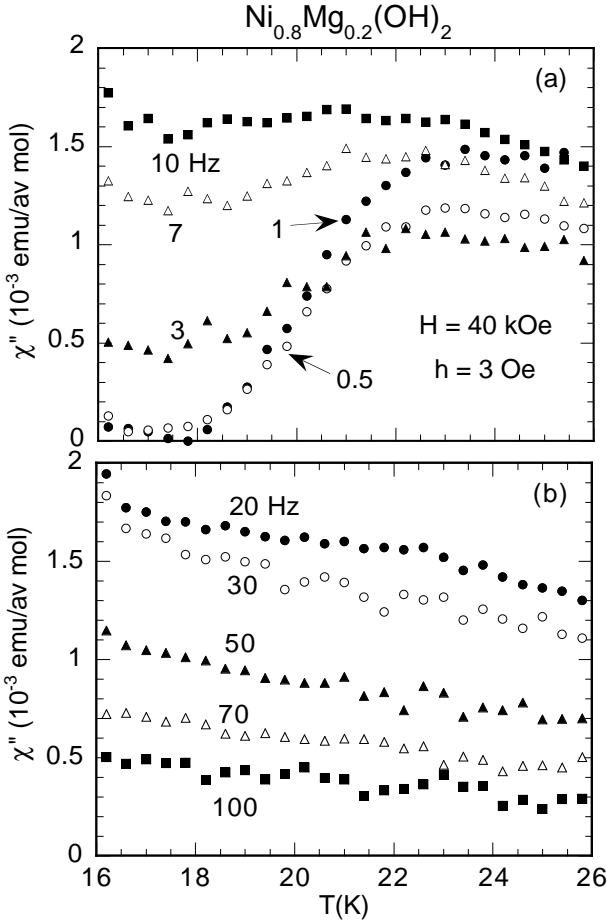


Fig. 11. (a) and (b)  $T$  dependence of  $\chi''$  at various  $f$  ( $0.5 \leq f \leq 100$  Hz).  $H = 40$  kOe.  $h = 3$  Oe.

in the Griffiths phase are nearly ordered and relax very slowly. The  $T$  dependence of the average relaxation time ( $\tau_G$ ) will be discussed in §5.5.

## 5. Discussion

### 5.1 Definition of $T_N(H)$

Before we discuss the  $H$ - $T$  phase diagram, it is instructive to explain how to determine the Néel temperature  $T_N(H)$ . In Fig. 12 we make a plot of the following characteristic temperatures which may be related to  $T_N(H)$ , as a function of  $H$  in the  $H$ - $T$  plane: the peak temperatures of  $\chi_{FC}$  vs  $T$ ,  $\chi_{ZFC}$  vs  $T$ ,  $d\chi_{FC}/dT$  vs  $T$ ,  $d\chi_{ZFC}/dT$  vs  $T$ ,  $\chi'$  vs  $T$ , and  $\chi''$  vs  $T$ , and local-minimum temperatures of  $\chi''$  vs  $T$  and  $\delta$  vs  $T$ . These characteristic temperatures can be classed into four groups, depending on  $H$  and  $T$ : (i) the peak temperatures of  $\chi_{FC}$ ,  $\chi_{ZFC}$ , and local-minimum temperature of  $\chi''$ , (ii) the peak temperature of  $\chi'$ , (iii) the peak temperatures of  $d\chi_{FC}/dT$ ,  $d\chi_{ZFC}/dT$ , and  $\chi''$ , and (iv) the local-minimum temperature of  $\delta$ . In an usual Ising antiferromagnet, the  $T$ -derivative of the DC susceptibility  $\chi_{\parallel}$  along the easy axis,  $(d\chi_{\parallel}/dT)$ , diverges at  $T_N(H)$ . The peak temperature of  $\chi_{\parallel}$  vs  $T$  is higher than  $T_N(H)$ . The magnetic heat capacity  $C_{mag}$  as well as  $\chi'$  and  $\chi''$  also show a peak at  $T_N(H)$ . Because of the Maxwell relation [ $(\partial S/\partial H)_T = (\partial M/\partial T)_H$ ], the  $H$ -derivative of  $C_{mag}$  is related to  $d\chi_{\parallel}/dT$ . Thus the first and fourth groups are not di-

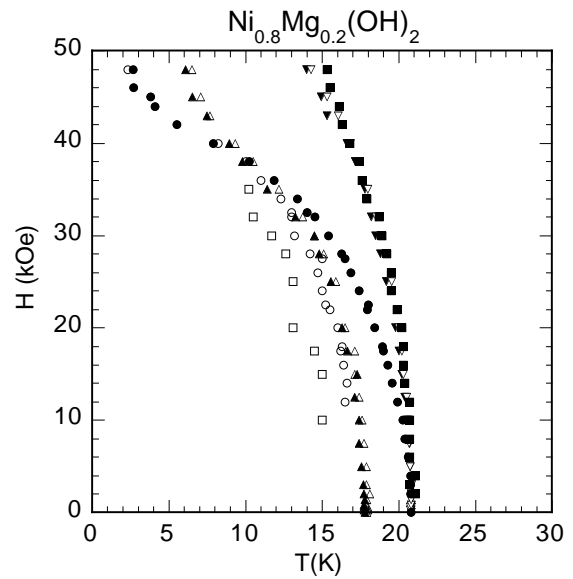


Fig. 12. Definition of  $T_N(H)$ . The following characteristic temperatures are plotted as a function of  $H$ : the peak temperatures of  $\chi'$  (●),  $\chi''$  (○),  $d\chi_{ZFC}/dT$  (▲),  $d\chi_{FC}/dT$  (△),  $\chi_{ZFC}$  (▼), and  $\chi_{FC}$  (▽), and local-minimum temperatures of  $\chi''$  (■) and  $\delta$  (□).

rectly related to  $T_N(H)$ . The second and third groups of our system may correspond to the critical lines denoted by the lines  $H_c$  and  $H_1$  (see Fig. 13). Similar behavior is observed in a 3D Ising antiferromagnet  $\text{FeBr}_2$ .<sup>24-28</sup> In  $\text{FeBr}_2$ , the data of  $C_{mag}$  vs  $T$ ,  $\chi'$  vs  $T$ , and  $\chi''$  vs  $T$  show peaks at  $T_N(H)$  along the line  $H_c$ , and the data of  $C_{mag}$  vs  $T$  and  $\chi''$  vs  $T$  show peaks at a critical temperature  $T_1(H)$  ( $< T_N(H)$ ) along the line  $H_1$ .

### 5.2 $H$ - $T$ phase diagram

Figure 13 shows the  $H$ - $T$  phase diagram of  $\text{Ni}_c\text{Mg}_{1-c}(\text{OH})_2$  with  $c = 0.8$ . It consists of the lines denoted by  $H_c$ ,  $H_1$ ,  $H_2$ ,  $H_3$ ,  $H_{\alpha}$ ,  $H_{\beta}$ ,  $H_{RSG}$ , and  $H_G$ , and two points denoted by a multicritical point  $P_m$  ( $T_m = 5.6$  K,  $H_m = 42$  kOe) and a critical point  $P_0$  ( $T_0 = 10$  K,  $H_0 = 38$  kOe). The features of the  $H$ - $T$  diagram are summarized as follows. (i) A spin-flop transition occurs around the critical point  $P_0$ . The line  $H_c$  connecting between  $P_0$  and  $T_N(c = 0.8, H = 0)$  ( $= 20.7$  K), is of the second order. (ii) The region enclosed by the extension of the lines  $H_c$ ,  $H_2$ , and  $H_3$  may be a spin-flop (SF) phase. (iii) The line  $H_1$  connects between the critical point  $P_0$  and a characteristic temperature ( $= 17.74$  K) at  $H = 0$ . The nature of intermediate phase between the lines  $H_1$  and  $H_c$  is not clear at present. Note that similar intermediate phase is observed in  $\text{FeBr}_2$ , where the transverse component of AF order parameter is enhanced on crossing the line  $H_1$ .<sup>28</sup> (iv) The line  $H_{RSG}$  is the boundary between the RSG and AF phases. This line corresponds to an Almeida-Thouless (AT) line between SG and PM phases.<sup>29</sup> (v) The line  $H_{SG}$  is the boundary between the SG and RSG phases (see §5.3). The region enclosed by the lines  $H_{SG}$  and  $H_2$  is the SG phase. (vi) The extensions of the lines  $H_{\alpha}$  and  $H_{\beta}$  may merge at the multicritical point  $P_m$ . The nature of the

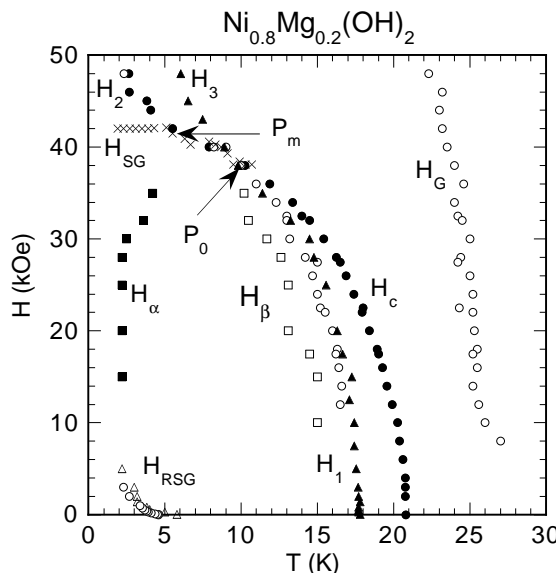


Fig. 13.  $H$ - $T$  phase diagram: peak temperatures of  $\chi'$  (●),  $\chi''$  (○),  $d\chi_{ZFC}/dT$  (▲), the characteristic temperatures  $T_\delta$  (■),  $T_{min}$  (□), and  $T_{RSG}$  (△) for  $\delta$ . The definition of lines  $H_c$ ,  $H_1$ ,  $H_2$ ,  $H_3$ ,  $H_\alpha$ ,  $H_\beta$ ,  $H_{RSG}$ ,  $H_G$ , the points  $P_m$  and  $P_0$  is given in the text.

lines  $H_\alpha$  and  $H_\beta$  will be discussed in §5.4. (vii) The line  $H_G$  is in the PM phase and is related to the Griffiths phase (see §5.5). The characteristic temperatures along the line  $H_G$  are lower than  $T_N(c = 1, H = 0)$  ( $= 26.4$  K) of the pure system. It slightly decreases with increasing  $H$ , reflecting the antiferromagnetic nature of the system. The line  $H_G$  is essentially different from a non-critical line for ferromagnetic short-range order where a characteristic temperature increases with increasing  $H$  in the PM region.

### 5.3 Field-induced spin glass phase

We compare the  $H$ - $T$  phase diagram for  $\text{Ni}_{0.8}\text{Mg}_{0.2}(\text{OH})_2$  (Fig. 13) with the predicted one shown in Figs. 1(a) and (b). The lines  $H_2$  and  $H_{SG}$  meet the extension of the line  $H_c$  at the multicritical point  $P_m$ . The line  $H_{SG}$  is the boundary between the RSG and SG phases. There is only a SG state in the SG phase, while the SG phase coexists with the AF phase in the RSG phase. The line  $H_{RSG}$ , which is the boundary between the RSG and AF phase, disappears above 5 kOe. If the line  $H_\alpha$  corresponds to the boundary between the RSG and AF phases, our  $H$ - $T$  diagram is in good agreement with the prediction shown in Fig. 1(a): the AF-RSG transition temperature increases with increasing  $H$ . The extrapolation of the line  $H_\alpha$  to the higher- $T$  side seems to intersect the multicritical point  $P_m$ . The nature of the line  $H_\alpha$  will be discussed in §5.4. Here we note that only  $\chi''$  exhibits an anomaly when crossing the line  $H_{SG}$  at fixed  $T$ .

The  $H$ - $T$  phase diagram for  $\text{Ni}_{0.8}\text{Mg}_{0.2}(\text{OH})_2$  is a little different from that of  $\text{Fe}_{0.552}\text{Mg}_{0.448}\text{Cl}_2$  which undergoes a metamagnetic transition around a multicritical point. In  $\text{Fe}_{0.552}\text{Mg}_{0.448}\text{Cl}_2$  the line  $H_{RSG}$  intersects the line  $H_c$  at the multicritical point  $P_m$ .<sup>14)</sup> There are two features

on the data of  $T_{RSG}(H)$  vs  $H$ . The critical temperature  $T_{RSG}(H)$  at low  $H$  increases with increasing  $H$ , enlarging the domain of existence of RSG phase. The temperature  $T_{RSG}$  starts to decrease at higher  $H$  before it meets the multicritical point. The former feature is in good agreement with the prediction from the molecular field theory, but the latter feature is rather different from the prediction.

Along the line  $H_2$  a striking reversal of the curvature of the line  $H_2$  is observed as  $H$  is increased above 42 kOe. Similar behavior is observed for  $\text{Fe}_c\text{Mn}_{1-c}\text{TiO}_3$  with  $c = 0.60$  and  $0.65$ .<sup>30,31</sup> The line  $H_2$  is considered to be associated with the Almeida-Thouless (AT) replica symmetry-breaking line. In fact the curvature of the line  $H_2$  seems to be similar to that of the line  $H_{RSG}$ . The reversal of curvature is understood within the framework of the mean field theory.<sup>5)</sup> The origin of the SG phase for  $c = 0.8$  is considered to be as follows.<sup>4)</sup> The dilution by nonmagnetic Mg introduces the competition between the intraplanar nearest neighbor (N.N.) FM interactions, the intraplanar next-nearest-neighbor (N.N.N.) AF interactions, and the interplanar N.N. AF interactions, which leads to the spin frustration effect.

## 5.4 Glassy phase

The nature of the irreversibility of susceptibility ( $\delta$ ) is discussed in relation to glassy phases in SG, RSG, Griffiths phases, and RF effect. Our results of  $\delta$  (see Figs. 3 and 4) are summarized as follows. (i) For  $H < 10$  kOe,  $\delta$  is always positive for  $1.9 \leq T \leq 30$  K. (ii) For  $H \leq 3$  kOe,  $\delta$  increases in two steps with decreasing  $T$ : a weak change at  $T_{RF}$  and a strong change at  $T_{RSG}$ . (iii) For  $H > 12.5$  kOe,  $\delta$  shows a negative local minimum at  $T_{min}$ . (iv) For  $10 \leq H \leq 25$  kOe,  $\delta$  shows a local maximum around the Griffiths temperature  $T_G(H)$  above  $T_N(H)$ . (v) At  $17.5 \leq H \leq 35$  kOe,  $\delta$  shows a drastic decrease with decreasing  $T$  below  $T_\delta$ , as well as a negative local minimum at  $T_{min}$ . (vi) For  $H \geq 38$  kOe,  $\delta$  becomes negative below 30 K and decreases with decreasing  $T$ . In the  $H$ - $T$  diagram of Fig. 13, we make a plot of  $T_\delta$ ,  $T_{min}$ , and  $T_{RSG}$  for each  $H$ , which forms the line  $H_\alpha$  for  $T_\delta$ , the line  $H_\beta$  for  $T_{min}$ , and the line  $H_{RSG}$  for  $T_{RSG}$ . The extension of the lines  $H_\alpha$  and  $H_\beta$  seems to join the multicritical point  $P_m$ . The transition temperature  $T_{RSG}(H)$  defined as the onset temperature of strong irreversibility in  $\delta$  is a little higher than the peak temperature of  $\chi''$  (see the inset of Fig. 3(a)). No RSG transition is observed above 5 kOe.

We note that the two step-like changes in  $\delta$  is also observed in the 3D Ising spin glass  $\text{Fe}_c\text{Mn}_{1-c}\text{TiO}_3$ . This system undergoes the P-AF and AF-RSG transitions at  $H = 0$ . The transition temperatures  $T_{RSG}(H)$  and  $T_N(H)$  are defined as the peak temperatures of magnetic diffuse neutron scattering, where the inverse spin correlation length has local minima.<sup>30)</sup> A series of magnetization measurements<sup>31)</sup> on  $\text{Fe}_c\text{Mn}_{1-c}\text{TiO}_3$  ( $0 < c < 0.41$ ) indicates that  $T_{RSG}(H)$  is not the onset temperature below which  $\delta$  become negative. The difference  $\delta$  exhibits a crossover from a weak irreversibility just below  $T_N(H)$  to a strong irreversibility at  $T_{RSG}(H)$ . The weak irreversibility is related to the RF effect and the strong irreversibility is related to the RSG transition. In

fact, Yoshizawa et al.<sup>30)</sup> have shown from the magnetic neutron scattering of  $\text{Fe}_{0.6}\text{Mn}_{0.4}\text{TiO}_3$  that the antiferromagnetic intensity and diffuse scattering suffer from the RF effect in the presence of  $H$ , in spite of the fact that  $\text{Fe}_{0.6}\text{Mn}_{0.4}\text{TiO}_3$  is not a diluted Ising antiferromagnet. The neutron scattering profile as well as the temperature dependence of the intensities exhibit pronounced history dependence between the FC and ZFC states below  $T_N(H)$ . The ZFC measurement shows a sharp transition to a long-range ordered AF state, while the FC measurement exhibits broadened transitions characteristic of domains (short range) being frozen below  $T_N(H)$ . The FC procedure causes the system to lose equilibrium and enter a metastable, frozen, domain state without long-range order.

How can we understand the anomalous behavior in  $\delta$  near the lines  $H_\beta$ ? The line  $H_\beta$  is qualitatively explained as follows. Numerical calculations<sup>7-11)</sup> based on the molecular field theory for a 3D diluted Ising antiferromagnet suggest that a region of AF long-range order and a region of glassy state exist in the  $H$ - $T$  plane. In the region of AF long-range order, the ZFC state has a lower free energy and in the region of glassy state the FC state does. de Almeida and Bruinsma<sup>11)</sup> have shown that the region of glassy state is truly separate phase. The glassy phase remains restricted to large  $H$ , where the strength of random field varies with  $H$ . The detail of the phase boundary between these two phases has been obtained by Ro et al.<sup>8)</sup> for the 3D diluted AF system with  $c = 0.7$ . The line  $H_\beta$  qualitatively coincides with this phase boundary. The origin of this line may be due to inhomogeneous internal field, which is given by  $H_{int} = H - NM$ , where  $N$  is the demagnetization factor. This internal field couples with the AF order parameter. If this field is strongly inhomogeneous, it may play the same role as the RF field. The line  $H_\alpha$  is not predicted from numerical calculations.<sup>7-11)</sup> The line  $H_\alpha$  may correspond to the boundary between the RSG and AF phases.

How does the random field effect occur in our powdered sample which are assumed to be formed of nanoparticles? The local magnetic field for spin inside each nanoparticle is described by  $H_i \cos \theta$ , where  $\theta$  ( $0 \leq \theta \leq 2\pi$ ) is the angle between the local magnetic field  $\mathbf{H}_i$  and the easy spin axis of each particle. The mean value of the effective field is  $[H_i]_{av} \langle \cos \theta \rangle = 0$ , while the variance of the effective field is  $[H_i^2]_{av} \langle \cos^2 \theta \rangle = [H_i^2]_{av}/2 = (H_R)^2/2$ , where  $\langle \cos^2 \theta \rangle = 1/2$  and  $H_R$  is the random field of the single crystal and is defined as  $H_R^2 = [H_i^2]_{av}$ .<sup>32)</sup> Thus the random field for the powdered system is  $H_R/\sqrt{2}$ . In this sense, the random field effect is still effective for the powdered system.

### 5.5 Griffiths phase

Experimentally, the existence of the unfrustrated clusters of spins is confirmed from the maxima of  $\delta$  vs  $T$  and  $\chi''$  vs  $T$  in the PM phase above  $T_N(c, H)$ . Such clusters may be in nearly ordered states, and fluctuates with large relaxation times. This phenomenon is understood as the occurrence of the Griffiths phase. Here we briefly describe the picture of the cluster dynamics in the Griffiths phase. In a dilute Ising ferromagnet with concentration  $c$ , a clus-

ter is defined as a compact region in which spins are connected with each other by bonds. Such clusters become quasi-ordered at temperatures below  $T_G$  and flips collectively with anomalous long characteristic times. The consequence of such processes is slow dynamics of the spin auto-correlation function  $q(t)$ , whose asymptotic form at a large time  $t$  is given by  $q(t) \approx \exp[-\lambda(\ln t)^{d/(d-1)}]$ ,<sup>33-35)</sup> where  $d$  is the dimension of the system and  $\lambda$  is a constant. This decay form is called the enhanced power law. Griffiths<sup>13)</sup> has shown that for a randomly site-diluted Ising ferromagnet with magnetic concentration  $c$ , the magnetization fails to be an analytical function of  $H$  for any temperature within the so-called Griffiths phase  $T_c(c, H) \leq T_G(H) \leq T_c(c = 1, H = 0)$ , where  $T_c(c, H)$  is the critical temperature at  $H$  for the diluted ferromagnetic system with the concentration  $c$ . In our system, Ni spins with Ising symmetry are ferromagnetically ordered in the same  $\text{Ni}_c\text{Mg}_{1-c}$  layer, where a part of  $\text{Ni}^{2+}$  spins is randomly replaced by nonmagnetic  $\text{Mg}^{2+}$  ions. Thus in the limit of weak AF interplanar interactions, our system is similar to the site-diluted Ising ferromagnet:  $T_N(c, H) \leq T_G \leq T_N(c = 1, H = 0)$ . Surprisingly the Griffiths phase is observed even for the pure system  $\text{Ni}(\text{OH})_2$ , where  $T_G(c = 1, H)$  is larger than  $T_N(c = 1, H = 0)$ . Such a Griffiths phase is also observed in a 3D antiferromagnet  $\text{FeCl}_2$ .<sup>16)</sup> For  $\text{FeCl}_2$ ,  $T_G(H)$  is between  $T_N(c = 1, H)$  and  $T_N(c = 1, H = 0)$ , which is different from that for  $\text{Ni}(\text{OH})_2$ . This behavior is explained in terms of fluctuating distributions of demagnetizing fields.

What is the nature of the Griffiths phase for  $\text{Ni}_{0.8}\text{Mg}_{0.2}(\text{OH})_2$ ? The absorption  $\chi''$  is related to the power spectrum of the magnetization fluctuation according to the fluctuation-dissipation theorem. As shown in Fig. 9(a), we find that  $\chi''$  shows a broad peak at  $T_G(H)$  between  $T_N(c = 0.8, H = 0)$  (= 20.7 K) and  $T_N(c = 1, H = 0)$  (= 26.4 K) for  $H \geq 10$  kOe. This broad peak shifts to the low- $T$  side with increasing  $H$ , reflecting the nature of antiferromagnetic fluctuations, but not ferromagnetic fluctuations. There is no anomaly in  $\chi'$  at any  $T$  above  $T_N(H)$ . As shown in Figs. 10(b) and 11(a), the broad peak at  $T_G(H)$  for  $H = 30$  and 40 kOe is strongly dependent on  $f$ . This peak shifts to the low- $T$  side with increasing  $f$  for  $0.5 \leq f \leq 10$  Hz and seems to disappear for  $f \geq 20$  - 30 Hz. If  $\chi''$  has a peak at  $\omega\tau_G = 1$  ( $\omega = 2\pi f$ ), then the corresponding characteristic relaxation time  $\tau_G$  can be estimated as  $\tau_G = (2\pi f)^{-1}$ . Figure 14 shows the  $T$  dependence of  $\tau_G$  thus obtained for  $H = 30$  and 40 kOe. Surprisingly the relaxation time  $\tau_G$  increases with increasing  $T$  in the limited  $T$  range. The value of  $\tau_G$  is anomalously large at  $T$  much higher than  $T_N(H)$ . Such a large  $\tau_G$  may be attributed to preferentially formed large spin clusters, leading to the field-induced Griffiths phase. The reason of the increase of  $\tau_G$  with increasing  $T$  is not clear at present.

Similar behavior is observed in  $\text{Fe}_{0.47}\text{Zn}_{0.53}\text{F}_2$ <sup>17)</sup> and  $\text{FeCl}_2$ .<sup>16)</sup> In  $\text{Fe}_{0.47}\text{Zn}_{0.53}\text{F}_2$ ,  $\chi'$  at  $f = 1$  Hz in the ZFC state shows a narrow peak at  $T_N(H)$  and a very broad main peak at  $T_G(H)$  [ $> T_N(c, H)$ ] for  $H \geq 30$  kOe. This feature is more pronounced as  $H$  is increased. In contrast,  $\chi''$  shows a sharp peak at  $T_N(c, H)$ . It extends an

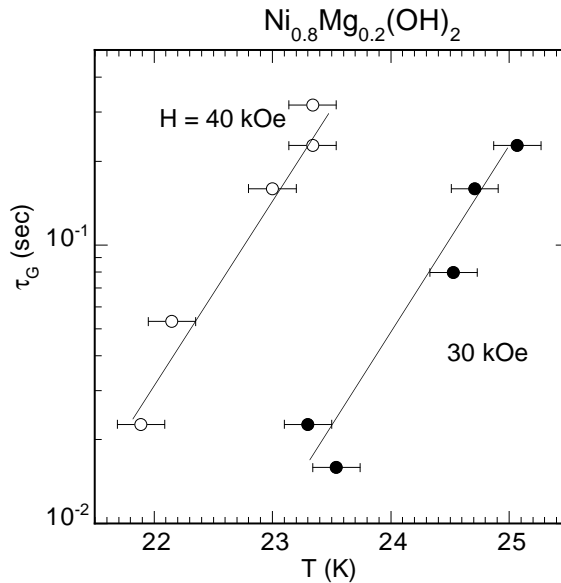


Fig. 14.  $T$  dependence of the relaxation time  $\tau_G$  for the Griffiths phase.  $H = 30$  and  $40$  kOe. The solid lines are a guide to eyes.

asymmetric flat tail for  $T_N(c = 0.47, H) < T < T_N(c = 0.47, H = 0)$ . In  $\text{FeCl}_2$ ,  $\chi''$  shows a broad peak at  $T_G(H)$  for  $H \geq 12$  kOe, where  $T_N(c = 1, H) < T_G(H) < T_N(c = 1, H = 0)$ . The absorption  $\chi''$  is strongly dependent on  $f$ . For example,  $\chi''$  at  $H = 18$  kOe has a peak at  $T_G(H)$  at  $f = 1$  Hz. However, this peak disappears at  $f = 0.1$  and  $10$  Hz. This result is in good agreement with our result.

## 6. Conclusion

The  $H$ - $T$  phase diagram of  $\text{Ni}_{0.8}\text{Mg}_{0.2}(\text{OH})_2$  consists of the RSG, SG, and AF phases. These phases meet a multicritical point  $P_m$ . A spin-flop transition occurs around the critical point  $P_0$ . These results are in good agreement with the theoretical prediction from the molecular field theory. The existence of the glassy phase in the AF phase and the Griffiths phase in the paramagnetic phase is also confirmed. Further studies will be required to understand the nature of the SG phase, glassy phase and Griffiths phase.

## Acknowledgment

The authors would like to thank T. Y. Huang for his assistance in SQUID magnetization measurements. The work at Binghamton was partially supported by the SUNY-Binghamton Research Foundation (240-9522A).

1) For a recent review of the theory and experiment of RFIM and spin glass, see A. P. Young: *Spin Glasses and Random Fields* (World Scientific, Singapore, 1998).

- 2) Y. Imry and S. K. Ma: *Phys. Rev. Lett.* **35** (1975) 1399.
- 3) S. Fishman and A. Ahalony: *J. Phys. C: Solid State Phys.* **12** (1979) L729.
- 4) M. Suzuki, I. S. Suzuki and T. Enoki: *J. Phys. Condensed Matter* **12** (2000) 1377.
- 5) H. Takayama: *Prog. Theor. Phys.* **80** (1988) 827.
- 6) Ya V. Fyodorov, I. Ya Korenblit and E. F. Shender: *J. Phys. Condensed Matter* **2** (1990) 1669.
- 7) C. M. Soukoulis, K. Levin, and G. S. Grest: *Phys. Rev. B* **28** (1983) 1495.
- 8) C. Ro, G. S. Grest, C. M. Soukoulis and K. Levin: *Phys. Rev. B* **31** (1985) 1682.
- 9) C. M. Soukoulis, G. S. Grest, C. Ro and K. Levin: *J. Appl. Phys.* **57** (1985) 3300.
- 10) G. S. Grest, C. M. Soukoulis, and K. Levin: *Phys. Rev. B* **33**, (1986) 7659.
- 11) J. R. L. de Almeida and R. Bruinsma: *Phys. Rev. B* **35**, (1987) 7267.
- 12) H. Yoshizawa and D. P. Belanger: *Phys. Rev. B* **30**, (1984) 5220.
- 13) R. B. Griffiths: *Phys. Rev. Lett.* **23**, (1969) 17.
- 14) J. Gelard, F. Bensamka, D. Bertrand, A. R. Fert, J. P. Redoules, and S. Legrand: *J. Phys. C: Solid State Phys.* **16**, (1983) L939.
- 15) P.-z. Wong, S. von Molnar, T. T. M. Palstra, J. A. Mydosh, H. Yoshizawa, S. M. Shapiro, and A. Ito: *Phys. Rev. Lett.* **55**, (1985) 2043.
- 16) Ch. Binek and W. Kleemann: *Phys. Rev. Lett.* **72**, (1994) 1287.
- 17) Ch. Binek, S. Kuttler, and W. Kleemann: *Phys. Rev. Lett.* **75**, (1995) 2412.
- 18) H. Deguchi, M. Aikawa, K. Ohtani, and S. Takagi: *J. Mag. Mag. Mater.* **177-81**, (1998) 87.
- 19) K. Zenmyo, H. Kubo, H. Deguchi, and S. Takagi: *Physica B* **284-288**, (2000) 1511.
- 20) T. Enoki and I. Tsujikawa: *J. Phys. Soc. Jpn.* **39**, (1975) 317.
- 21) M. Lederman, J. V. Selinger, R. Bruinsma, R. Orbach, and J. Hammann: *Phys. Rev. B* **48**, (1993) 3810.
- 22) I. S. Suzuki, T. Y. Huang, and M. Suzuki: *Phys. Rev. B* **65**, (2002) 224432.
- 23) T. Enoki and I. Tsujikawa: *J. Phys. Soc. Jpn.* **46**, (1979) 1027.
- 24) M. M. P. de Azevedo, Ch. Binek, J. Kushauer, W. Kleemann, and D. Bertrand: *J. Mag. Mag. Mater.* **140-144**, (1995) 1557.
- 25) H. Aruga Katori, K. Katsumata, and M. Katori: *Phys. Rev. B* **54**, (1996) R9620.
- 26) K. Katsumata, H. Aruga Katori, S. M. Shapiro, and G. Shirane: *Phys. Rev. B* **55**, (1997) 11466.
- 27) O. Petracic, Ch. Binek, W. Kleemann, U. Neuhausen, and H. Lueken: *Phys. Rev. B* **57**, (1998) R11051.
- 28) Ch. Binek, T. Kato, W. Kleemann, O. Petracic, D. Bertrand, F. Bourdarot, P. Burlet, H. Aruga Katori, K. Katsumata, K. Prokes, and S. Welzel: *Eur. Phys. J. B* **15**, (2000) 35.
- 29) J. R. L. de Almeida and D. J. Thouless: *J. Phys. A* **11**, (1978) 983.
- 30) H. Yoshizawa, H. Mori, H. Kawano, H. Aruga Katori, S. Mitsuhashi, and A. Ito: *J. Phys. Soc. Jpn.* **63**, (1994) 3145.
- 31) H. Aruga Katori, T. Goto, S. Ebii, and A. Ito: *J. Mag. Mag. Mater.* **104-107**, (1992) 1639.
- 32) J. A. Mydosh: *Spin glasses: an experimental introduction* (Taylor and Francis, London, 1993).
- 33) T. Komori and H. Takayama: *J. Phys. Soc. Jpn.* **66**, (1997) 1472.
- 34) A. J. Bray: *Phys. Rev. Lett.* **59**, (1987) 586.
- 35) A. J. Bray: *Phys. Rev. Lett.* **60**, (1988) 720.